A Density-Functional Study of Heterometallic Cr-Based Molecular Rings

V. Bellini*,† and M. Affronte†,‡

CNR-Institute of NanoSciences - S3, via Campi 213/a, 41125 Modena, Italy, and Dipartimento di Fisica, Universita di Modena e Reggio Emilia, via Campi 213/a, 41125 Modena, Italy

Received: January 25, 2010; Revised Manuscript Received: October 1, 2010

We present a density-functional theoretical investigation of the electronic and magnetic properties of octametallic Cr-based molecular antiferromagnetic rings. The presence of the divalent magnetic ion M unbalances the charge and the spin of the parent Cr_8 ring, leading to a finite total spin in the molecules. Results are presented for Cr_8, i.e., $[Cr_8F_8(O_2CH)_{16}]$ (**1**), and for Cr_7M rings belonging to two different derivatives, i.e., $[Me_2NH_2][Cr_7MF_8(O_2CH)_{16}]$, with M = Ni, Mn, Fe, and Cu, and Me═CH_3 (**2**, "green" derivative), and $[Cr_7NiF_3(C_6H_{10}NO_5)(O_2CH)_{15}(H_2O)]$ (**3**, "purple" derivative). Exchange interaction parameters have been extracted from broken-symmetry calculations and compared with the available experiments; in agreement with them, we find that exchange parameters are rather similar in the two derivatives, although somewhat larger in the "purple" derivative. The analysis of the electronic properties shows some differences depending on M, in particular in the size of the highest occupied molecular orbital to lowest unoccupied molecular orbital (HOMO−LUMO) gaps. For all the "green" rings we observe that the HOMOs are localized on the divalent ion site, while the HOMOs for the "purple" Cr_7Ni have a more delocalized nature; LUMOs, instead, are, except for "green" Cr_7Cu, localized on the Cr atoms opposite to the M site. We discuss how these findings may show up in terms of an asymmetric $I-V$ curve in molecular junctions working in the sequential tunneling regime, or help in discerning the orientation of the molecules with respect to a surface, in scanning tunneling experiments.

Introduction

Magnetic coordination molecular clusters have been increasingly studied in the past years, emerging as candidates for applications in magnetic information storage and processing. They also offer a unique playground to observe quantum phenomena at the mesoscopic scale, as step-like hysteresis curves due to quantum tunneling of the magnetization[1] or quantum coherence.[2] If high-spin molecules with large anisotropy barriers can be exploited to host one magnetic bit, low-spin molecules, with $S = 1/2$, can on the other hand be envisaged to encode qbits. Following the pioneering theoretical work of Loss and co-workers,[3,4] heterometallic antiferromagnetic (AFM) rings have been primarily and intensively investigated in the latter years for alluring application in quantum information technology;[5−9] moreover, synthetic chemistry is now able to build almost at will supramolecular-organized low-spin AFM rings with tailored magnetic properties, as demonstrated by the work of Winpenny's group in Manchester.[8,10]

Besides the ferric wheels, an important role has been surely played by the Cr family of the AFM ring, and within it, by the Cr_7Ni rings. Upon substiting one Cr^{3+} ion in the parent Cr_8 molecule (characterized by a dominant AFM exchange coupling between the Cr magnetic moments, and consequently by an $S = 0$ ground state[11]) with a divalent nonmagnetic, such as Cd^{2+} or Zn^{2+}, or magnetic, as Ni^{2+}, Fe^{2+}, Mn^{2+}, or Cu^{2+}, ion, a total spin $S \neq 0$ in the ground state is found. In the case of Cr_7Ni rings, the ground state is in very good approximation a Kramer doublet, being that the single-ion anisotropy is very small. A recent study by Corradini et al.[12] showed that isolated Cr_7Ni rings are stable on the surface, that is, the functionalization and most importantly the grafting procedure does not destroy the magnetic features of deposited Cr_7Ni rings, although a certain renormalization of the exchange interaction parameters arise from possible distortion of the rings.[13] As a matter of fact, this point is crucial in view of charge transport experiments, either placing the molecule between two leads and or depositing and addressing it with local scanning probes, which imply the use of molecules robust enough to preserve their magnetic properties and, in first row, their own molecular structures during the grafting procedure. If the experimental characterization of the magnetic properties of Cr_8 and of the substituted Cr_7M family, namely for M = Cd, Zn, Ni, Mn, Fe, and Cu, can be found in the literature,[14−17] no theoretical study from first-principles has been attempted so far, excluding the parent Cr_8 molecule.[18] The electronic and magnetic properties of Cr_8 have been studied by the authors[18,19] by density-functional theory (DFT) using an augmented plane wave (APW) basis set (implemented in the Wien2K code[20]), method **I** from now on, and the possibility of replicating the property of the full molecule by a simplified linear chain model has been also discerned.[13,21] Transport through homometallic spin rings has been predicted from Lehmann and Loss,[22] by means of a theoretical work grounded on model Hamiltonians, to show interesting properties in the case of AFM coupling between the spins in the ring. The study from first-principles of these rings can give further insight and supply indications on how heterometallic Cr rings are likely to behave when allowing a current to flow through them; special attention must also be devoted to the spin character of the electronic levels, which can act as spin-polarized transport channels.[23]

We present in the following a density-functional characterization of the electronic and magnetic properties of substituted

* To whom correspondence should be addressed. E-mail: valerio.bellini@unimore.it.
† CNR-NANO-S3, Modena.
‡ University of Modena and Reggio Emilia.

10.1021/jp107544z
Published on Web 10/29/2010

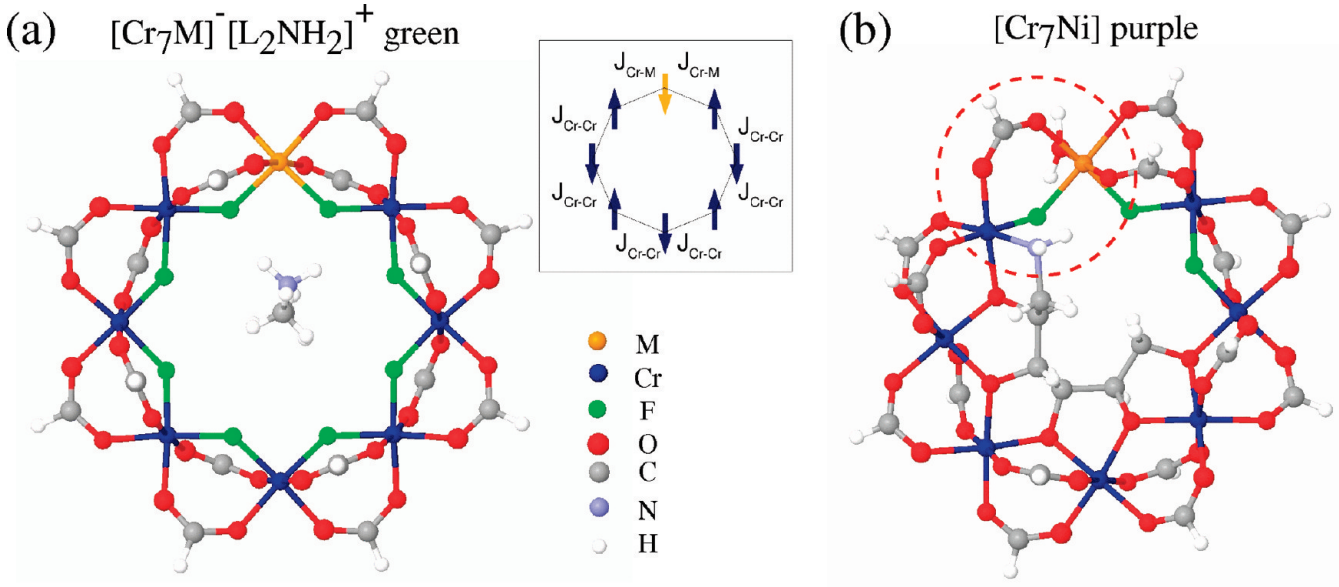

Figure 1. Color-coded molecular representation of the (a) derivative **2** and (b) derivative **3** (for details see the text); in the inset of panel a, the magnetic exchange interaction parameters J_{Cr-Cr} and J_{Cr-M} are sketched, where the up and down arrows represent the sign of the transition metal ion magnetic moments in the AFM state, when the substituting atom is Ni or Cu (the up arrows are aligned to the total spin of the molecule, defined as positive). L in panel a is, in our case, a methyl group $(CH_3)^+$ (see text).

Cr_7M rings, with M = divalent magnetic ion, i.e., Ni, Mn, Fe, and Cu, by using a Gaussian basis set code implemented in the NWChem quantum chemistry package,[24] method **II** from now on. Test calculations are also performed for the parent Cr_8 molecule in order to compare how different basis-sets (APWs and gaussians) and beyond local density approximation (LDA) functionals (LDA+U and B3LYP) perform in the study of the electronic and magnetic properties of this class of coordination molecular clusters. The detailed analysis of the electronic properties of heterometallic rings suggest that, in the case of transport in the resonant tunneling regime, it is possible, by selecting the resonant channels by bias voltage tuning, to attain information on the geometrical configuration of the ring−lead or ring−surface contacts, and, possibly, to spot the substituting M atom.

Systems and Computational Details

There are two derivatives of octa-metallic Cr-based substituted molecular rings. The first derivative, **2**, is characterized by having two pivalate and one fluorine bridging ligands connecting each metal pair, as much as the homometallic parent molecule, Cr_8; the presence of a substituting divalent M^{2+} ion in place of a Cr^{3+} ion leads to an imbalance of the charge in the ring of one formal negative charge $-e$, which, in order to separate and stabilize the molecule, is counterbalanced by a cation, an alkyl chain with different possible length, placed in the middle of the ring. The cation interacts with two fluorine atoms through three NH···F hydrogen bonds. These type of rings have been labeled as "green", after the color of the molecular crystals, and have been the ones initially and more systematically studied; synthetical techniques have succeeded in substituting both divalent nonmagnetic and paramagnetic ions. The second derivative, **3**, named "purple", instead is characterized by larger modification from the Cr_8 structure, where five out of eight fluorine bridges are replaced by a penta-deprotonated glucamine bridge, leading to a distortion of the almost perfect Cr octahedra.[25] Here, the imbalance in the charge, which leads to the divalent ion substitution, is given by the glucamine, which has a formal charge of $-e$, because of the presence of a four-coordinated N atom. Each magnetic ion is connected by the next magnetic ion in the ring by three (two pivalate and one fluorine) bridges except the substituting M ion and the nearby Cr ion on the side of the glucamine; the six-coordination of M is reached with bonding to a water molecule, while the nearby Cr ion completes its shell bonding to the glucamine (this region is highlighted by a red circle in Figure 1b). Both derivatives can be exploited as building blocks for any sort of supramolecular structure (dimers, trimers, etc.) with tailored properties.[9,25]

In order to relieve the computational cost, we have adopted the so-called "hydrogen termination" expedient, that is, we have replaced methyl groups CH_3 by isovalent H atoms; applying this procedure twice (see ref 18 for further details) the pivalic groups $C-(CH_3)_3$, which are attached to the C atom of each carboxylate bridges can be replaced by isovalent single H atoms. In addition, for **3**, a methyl group CH_2CH_3 in the coordination of N belonging to the glucamine bridge has been similarly substituted with a H atom. In the case of **2**, we have considered the smallest possible alkyl chain, i.e., $[Me_2NH_2]^+$, while in real molecules counterions of the type $[L_2\ NH_2]^+$, with L = Me, Et, Bu, etc. have been found.[26] Following this route, we attain the three formula units $[Cr_8F_8(O_2CH)_{16}]$ (Cr_8 in short), $[Me_2NH_2]$, and $[Cr_7MF_8(O_2CH)_{16}]$, with M = Ni, Mn, Fe, and Cu, and Me═CH_3 (depicted in Figure 1a, derivative **2**), and $[Cr_7NiF_3(C_6H_{10}NO_5)(O_2CH)_{15}(H_2O)]$ (depicted in Figure 1b, derivative **3**). The carboxylate groups that mediate, together with the fluorine one, the exchange interaction between the magnetic ions are barely affected in their electronic properties by the approximation discussed above; the presence of the organic matrix surrounding the magnetic core turns off intermolecular dipolar magnetic interaction between the rings, and this effect is reproduced in theoretical calculations either by inserting vacuum space around the rings in a supercell calculation, or by studying isolated molecules with real space methods. Although we will concentrate mainly on members of derivative **2**, we also present, for completeness, the characterization of Cr_7Ni ring **3**.

The presence of a substituting divalent ion disrupts the symmetry present in the Cr_8 rings; this, together with the

presence of the counterion (for **2**) or of the glucamine bridge (for **3**), leads to a total of 91 and 96 inequivalent atoms, respectively. In earlier articles, we have studied Cr cyclic structures by means of method **I** described in the Introduction; static correlation effects have been included by means of the LDA+U method,[27,28] the inclusion of which has been shown to improve the comparison with experimental data.[18,29,30] Since augmented plane wave methods are computationally not efficient in the absence of symmetry, we will tackle the study of heterometallic rings with method **II** described in the Introduction, which relies on a localized Gaussian basis set. In order to obtain trustworthy results, the B3LYP hybrid exchange-correlation functional has been considered, together with Ahlrichs valence triple-ζ (VTZ) basis set for the transition metal ions, and Ahlrichs valence double-ζ (VDZ) basis set for the rest of the elements.[31] The B3LYP functional is largely used nowadays in studying molecular structures, and lately also in the solid state, where it has been shown to lead to results comparable to the ones obtained by the LDA+U method in the case of strongly correlated transition metal oxides[32−34] and magnetic molecules.[29] Calculations have been performed in the absence of spin−orbit coupling. Low-spin broken-symmetry (BS) magnetic configurations have been reached with the aid of constrained density-functional method (C-DFT) as implemented by van Voohris et al.;[35,36] costraining the spin moments on different magnetic ions, we could impose Ising-like configurations with tailored distributions of the ionic spins, and using these calculations as starting initial guesses, we can proceed with relaxing the electronic degrees of freedom until convergence of the total energy for the desired BS spin state is reached. In this way, states with whatever spin-multiplicity and spin distribution can be obtained with relatively low cost, and exploited to extract exchange interaction parameters; the standard method, as opposed to the "non-projected" one proposed by Ruiz,[37] has been used throughout the paper, where J values are extracted by the total energies differences of Ising-like BS magnetic states (see more details in ref 18 in the case of Cr_8).

Finally, for all the structures, we have performed a full structural optimization until residual forces on each atom were below a few milli-Rydbergs per atomic unit. Upon force minimization, the structures are only weakly modified, both in bond angles and bond distances; most of the relaxation happens for the coordination shell of the M atom, in particular for the Cu atoms, for which energy gain due to Jahn−Teller distortion is higher. When not stated explicitly, the data discussed in the paper are relative to the optimized structures.

Results

APWs+GGA+U vs Gaussians+B3LYP Approaches: The Case of Cr_8 (1). In the Cr_8 rings, the dominant AFM exchange coupling between the Cr moments leads to a ground state with total spin $S = 0$. We present in Figure 2 a comparison between the total density of states (DOS) of Cr_8 obtained by the Wien2k code and GGA+U functionals (method **I**) and the NWChem code with B3LYP functionals (method **II**) in a broad energy range [the energy zero is set to the highest occupied energy level]; the use of generalized gradient approximation (GGA) instead of LDA only has the effect of requiring a smaller value of U, since the gradient of the electron density also enters in the functional, and a bit more of mean-field correlation is considered with respect to LDA. We have here performed the calculations for the experimentally determined X-ray structure. The agreement between the two DOSs is remarkable, and the only major difference is the larger highest occupied molecular orbital (HOMO) to lowest unoccupied molecular orbital (LUMO) gap found with method **II**, which amounts to 5.5 eV, while the value obtained by method **I** is around 4 eV, obtained considering $U_{Cr} = 2.7$ eV (Hubbard parameter) and $J_{Cr} = 0$ eV (exchange parameter). A larger value of U (or $U-J$) would give a larger HOMO−LUMO gap, without worsening the agreement between the calculated and the fitted-from-experiments value of the Heisenberg exchange parameter J acting between the Cr atoms, which was chosen as the major figure of merit for the choice of U, as will be discussed below. Comparison with Figure 6 in ref 18, where the partial DOS projected onto the different chemical elements and orbitals are also plotted, indicates that Cr-occupied d orbitals are mainly restricted in the energy window between −0.5 eV and the HOMO level. Although some small shifts in the major peak are observed, the width of the mayor peaks compare well, especially in the region of interest, around the HOMO−LUMO gap.

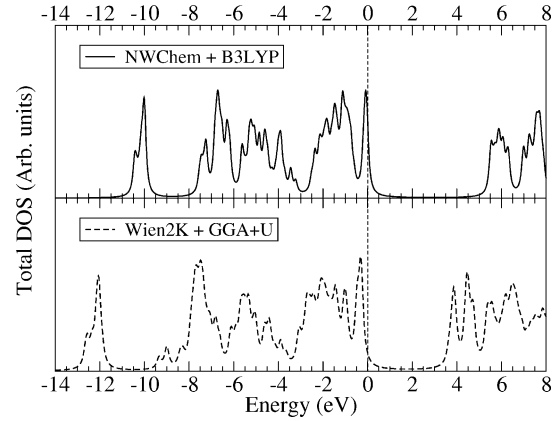

Figure 2. Comparison of the total DOS of Cr_8, as obtained by the two computational methods described in the text, for experimentally determined atomic positions.

The magnetic properties of most molecular magnets can be fairly well described by considering a pure spin Hamiltonian with different magnetic interaction terms, decoupling spin, and electronic degrees of freedom. Parameters describing such a Hamiltonian are usually inferred by mapping onto experimental data obtained by a variety of techniques, ranging from specific-heat to magnetization, electron paramagnetic, or nuclear magnetic resonance experiments. In the systems in which we are interested, the only relevant terms that characterize spin model Hamiltonians are the isotropic Heisenberg exchange interaction and crystal field-induced anisotropy terms. Since we have not considered spin−orbit coupling in our calculations, the latter terms vanish. In the case of Cr_8, the magnetic interactions in the ring can be described by a single exchange parameter J_{Cr-Cr}, and the total energy of different BS spin distribution can be mapped on a simple isotropic Heisenberg Hamiltonian. By subtracting total energies relative to the ground-state AFM ($S = 0$) and the highest ferromagnetic (FM, $S = 12$) configurations, where all the Cr $S = 3/2$ spins are aligned parallel, we can extract the exchange interaction parameter J_{Cr-Cr}. Values obtained by method **II** overestimate by a factor of 2 the values inferred from experiments (3.2 meV vs 1.5 meV), in agreement with the experience reported in the literature whenever the B3LYP functional and standard total energy difference methods are considered, while by using method **I** we obtained a smaller value, i.e., $J_{Cr-Cr} = 2.1$ meV.[18] Overall, the above results indicated that the two methods give similar results. The good comparison between the two exchange-correlation potentials, i.e., GGA+U and B3LYP, on the magnetic properties in

TABLE 1: The Nominal Electronic Configuration of the M Atoms, the Values of the M Magnetic Moments (in μ_B), the Total Spin, and the Values of the HOMO−LUMO Gaps (in eV) for Cr_8 and Cr_7M, M = Ni, Mn, Fe, and Cu Rings of Derivative 2, in the AFM State

	electr. config.	m (M)	S_{TOT}	HOMO−LUMO gap
Cr	$3d^3$	2.9	0	4.0
Ni	$3d^8$	1.7	1/2	4.2
Mn	$3d^5$	4.6	1	3.0
Fe	$3d^6$	3.8	1/2	2.1
Cu	$3d^9$	0.8	1	3.4

molecular system is a general finding, and other works in the literature support this observation.[38,39] The systematic study of the Cr_7M molecules presented below will be carried out exclusively by employing method **II**.

Cr_7M Molecular Rings of Derivative 2. ***Magnetic Properties.*** The nominal valence electronic configuration, the local spin magnetic moments (as calculated from a Mulliken population analysis) of the M atoms, the total spin attained by the ring, and the electronic gap in the AFM state (that is, where the Cr and M atoms are antiferromagnetically arranged in the ring) are listed in Table 1 for Cr_8 and Cr_7M, with M = Ni, Mn, Fe and Cu. The data presented here are relative to the optimized structures. Such an AFM state is, in all the cases, except for M = Cu, the calculated ground state of the molecules, as it will be discussed later in the text. In Figure 3, spin densities isosurfaces with values of ± 0.01 $e^-/a.u.^3$ are reported, where different colors correspond to the two signs of the spin-polarization, up and down. Here, up and down refer to the sign of the spin channel with respect to a positive total spin of the molecule, i.e., +1/2, for Cr_7Ni and Cr_7Fe, and +1, for Cr_7Ni and Cr_7Fe. We speak in the following sections on the majority and minority spin channel for the M d orbitals, after their occupation; the majority channel for nearly filled d orbitals, e.g., for Ni and Cu ions, is of spin down character, since Ni and Cu spins are, in the AFM state, antialigned (down) to the total spin of the molecule, while it has spin up character for nearly half-filled d orbitals, e.g., for Mn and Fe, where the spins of Mn and Fe are aligned (up) to the one of the molecule. This is the reason why, for Cr_7Ni and Cr_7Cu rings, colors of isosurfaces on the Cr spins are opposite to the ones for Cr_7Mn and Cr_7Fe. The three-dimensional shape of the spin densities is directly related to the symmetry of the magnetic orbitals. In the case of slightly distorted orthorhombic coordination, the transition metal d orbitals are split by the crystal field in two major blocks, with t_{2g}-like (lower energy) and e_g -like (higher energy) symmetries. Cr^{3+} has nominally only three electrons in the occupied d orbitals, so that only the t_{2g}-like states are spin-polarized, and since their lobes extend around the diagonals of the orthorhombic axes, their spatial distribution attains a cubic shape. For what concerns the divalent ions, Mn, Fe, Ni, and Cu have nominally 5, 6, 8, and 9 electrons in the d orbitals, respectively; Mn thus has both t_{2g}-like and e_g-like states polarized (sphere-shaped spin density), Fe has four out of five d orbitals spin polarized (a less perfect sphere-shaped spin density), Ni has the t_{2g}-like completely occupied and the two e_g-like states spin polarized (star-shaped spin density), and Cu has only the highest d level spin-polarized, which turns out to be of d_{z^2} e_g-like symmetry. In fact, for Cr_7Cu, structural optimization leads to a compressed Jahn−Teller effect (rare but possible), which stabilizes the $d_{x^2-y^2}$ e_g-like orbital, lowering its energy, and leaving the d_{z^2} e_g orbital higher in energy, and spin-polarized in a $3d^9$ electronic configuration. Although most of the spin polarization is localized on the transition-metal d-orbitals, a small spin-polarization is also induced on the neighboring O and F atoms. Such spin polarization/delocalization induces a spin splitting in the nuclear levels of O and F ions and hyperfine fields ranges between 3 and 6 T at nuclei positions.[40] In the presence of a finite nuclear spin, interaction between the electronic and nuclear spins is responsible for the decoherence effect as described in ref 19 in the case of Cr_7Ni.

In first approximation, only two different Heisenberg interaction parameters, namely, J_{Cr-Cr} and J_{Cr-M}, as depicted in the inset of Figure 1a, can be considered to replicate the magnetic properties of Cr_7M within a spin model Hamiltonian; in fact, the size of the next-nearest neighbor metal−metal magnetic interaction has been evaluated within a simplified chain model of Cr_8, and values on the order of 0.2 meV have been extracted, being 1 order of magnitude smaller than nearest neighbor ones, and can thus be savely neglected.[41] The isotropic spin Hamiltonian thus attains the form

$$H = J_{Cr-Cr}\sum_{i=1}^{6} S_{Cr}^{i}\cdot S_{Cr}^{i+1} + J_{Cr-M}\{S_{Cr}^{7}\cdot S_{M}^{8} + S_{M}^{8}\cdot S_{Cr}^{1}\} \quad (1)$$

where the nominal spin of Cr and M, i.e., Cr = 3/2, Ni = 1, Mn = 5/2, Fe = 2 and Cu = 1/2, will be used. In light of the fact that we have two parameters to be determined (three if we count the electronic constant term that is subtracted out whenever differences of total energies are performed), while having many possible magnetic configurations to map to, the system is clearly overdetermined. We decided to start from the two opposite configurations, namely the AFM and FM ones, the latter being the state with higher multiplicity, and to individually flip the moments on the divalent M ion or on the opposite Cr ion with respect to the ring, obtaining in total six different spin distribution states. We then averaged over the Js obtained from the $6!/(6-3)!3! = 20$ subsystems of three equations chosen out of the six possible ones. The exchange interaction parameters extracted as described above are listed in Table 2, together with the available experimental data. Calculations for the Cr_8 parent molecules give a value of $J_{Cr-Cr} = 3.9$ meV for the optimized geometry, not far from the values of J_{Cr-Cr} inferred from the substituted rings (3.3 meV), in agreement with the experimental evidence that substitution of one Cr atom with a divalent one does not modify the exchange interaction between the other Cr spins. Susceptibility and inelastic neutron spectroscopy experiments predict a value of around 1.5 meV for J_{Cr-Cr}, and very similar values (slightly smaller or larger, depending on the substituting atom and on the technique), for J_{Cr-M}. Our calculation predicts somewhat larger variations in J_{Cr-M}; most notably for Cr_7Cu, an FM J_{Cr-Cu} interaction is found.

Rings of derivative **2** are characterized by the disordered nature of the M site over all eight of the possible metal sites, as discussed in the original paper of van Slageren et al.[11] In other words, a clear preference between the eight possible metal positions for the substituting divalent atom is not observed in X-ray refinements. The relative position between the M sites and the alkyl counterion inside the ring, i.e., where the substituting atom sits as compared to the three NH···F hydrogen bonds, is also impossible to determine. In order to investigate this issue, total energy calculation might be of help. We indeed find that, by fully minimizing the structures (ring+cation), a gain of energy of more that 0.4 eV (very similar values have been found for different M) is obtained if the divalent ion

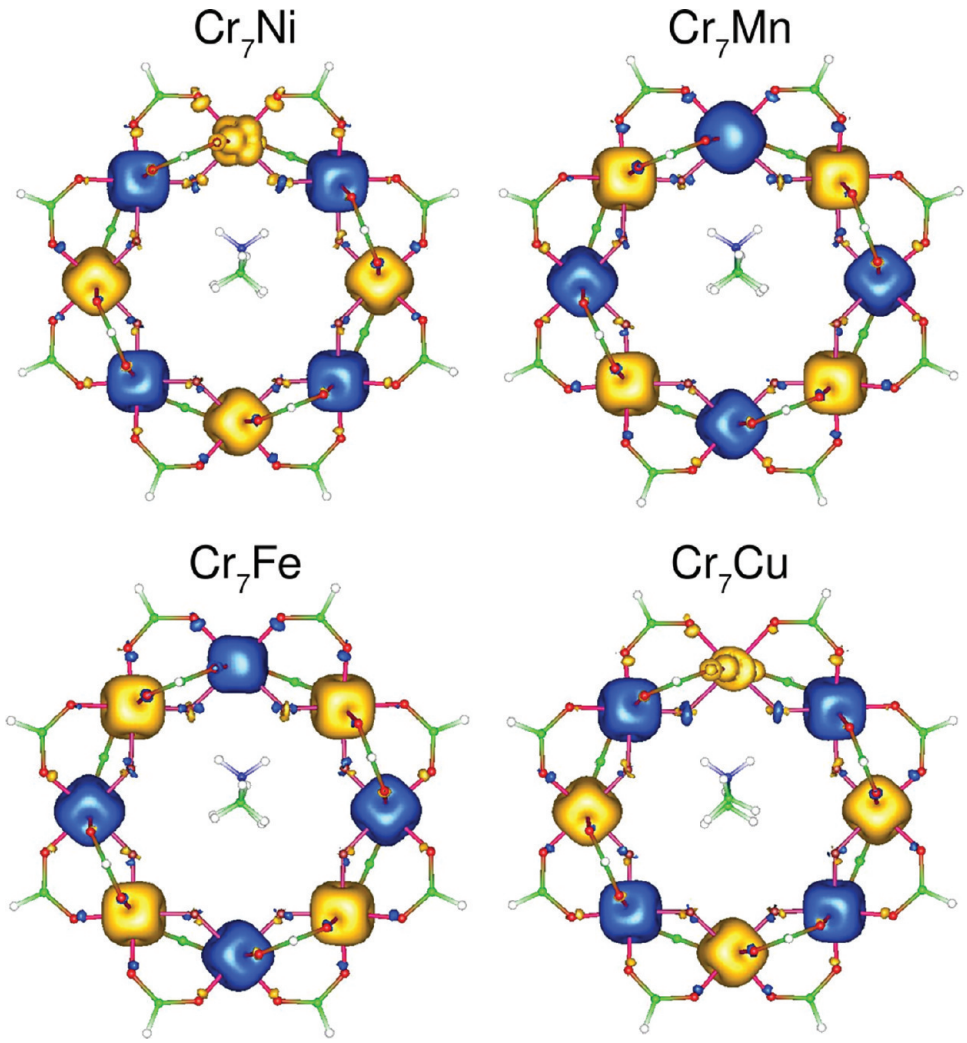

Figure 3. Isosurface plots of the electron spin density in Cr_7M, M = Ni, Mn, Fe, and Cu rings of derivative **2** in the AFM state (isovalues of ±0.01 electrons/a.u. have been used); different colors correspond to the positive (blue) and negative (yellow) values of the spin density, relative to the total spin of the molecule in the AFM state, which is set to positive (see text).

TABLE 2: Exchange Interaction Parameters (in meV) for Cr_7M, M = Ni, Mn, Fe, and Cu for the Optimized Structure

	theory		exp		
M atom	J_{Cr-M}	J_{Cr-Cr}	J_{Cr-M}	J_{Cr-Cr}	ref.
Ni	0.5	3.3	1.7	1.5	15
			1.3	1.4	51
Mn	1.3	3.3	1.4	1.5	15
Fe	2.2	3.3	1.1	1.1	17
			0.8	1.5	51
Cu	−1.7	3.3	1.6	1.5	16
			1.5	1.5	51

substitutes in one of the two metal sites connected to the F atoms hydrogen-bonded to the alkyl counterion, as compared to the case of substituting a metal site on the opposite side of the ring. This is a strong indication that the cation orients itself toward the position of the substituting ion. We observe further variations in the *J*s (calculations not shown), in the case where we place the divalent ion outside its minimum position. But, considering that measurements are performed at low temperatures, it is reasonable to assume that the structural conformation of the ring would be the one given by our ground-state calculations.

Finally, when discussing Table 2 we have to consider that *J*s in the Cr rings are rather small, and that deviations of several milli-electron volts is normally observed in other coordination compounds between theoretical and experimental values. An intrinsic source of errors in DFT methods is the spin-contamination issue, which arises when spin states other then the one with the highest multiplicity are calculated with the BS approach. Rudra et al.[42] have extensively addressed this issue, and show that *J*s extracted by C-DFT states, instead of BS states, compare better with experiments, because of the reduction in delocalization of the electrons; the choice of the "fragment" of molecule on which the spin constraint is imposed is rather critical in this respect, and it is not well-defined in the case of single-atom bridges, i.e., fluorine bridges in our case. The rings of derivative **2** are charge-balanced by the alkyl counterion placed in the middle of the ring, and the localization of such formal charge $-e$ on the ring is somewhat ensured by the hydrogen bonds between the alkyl counterion and the F atoms of the ring; another possible source of error that can enter in our calculation is thus the approximate treatment in the B3LYP functional of such hydrogen bonds. Calculations performed with more refined ab initio multideterminantal methods would be required to investigate this issue, although the systems studied here are rather large, and unfavorable scaling of the computational effort might prevent for the time being a systematic study of these molecules.

Electronic Properties. We now discuss the electronic properties of substituted rings, keeping an eye on possible ways to exploit them in measurements or applications. We present in

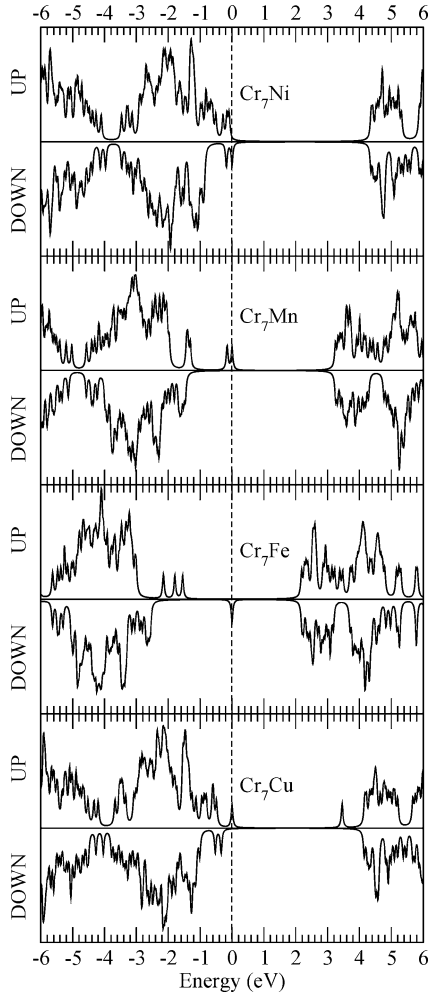

Figure 4. Spin polarized DOS for Cr_7M, M = Ni, Mn, Fe, and Cu rings of derivative **2**.

Figure 4 total DOS for up (↑) and down (↓) spin channels of Cr_7M rings. Several features are remarkable and worth being discussed. The electronic gap calculated for the optimized structure of Cr_8 is 4.0 eV (as compared to the 5.5 eV value obtained for the experimental structure, discussed in a previous section). In the case of Cr_7M, only for nearly filled M d orbitals do the majority spin levels deepen in energy enough to hybridize with the Cr occupied *d* orbitals, preserving the gap that would be intrinsic to Cr *d* orbitals, while in the case of nearly half-filled M d orbitals (M = Mn and Fe), the majority orbitals are higher in energy than the Cr ones, and the HOMO−LUMO electronic gap is reduced, in particular for M = Fe. Second, HOMOs are mainly of M-d + O-p hybrid character for all the rings, while LUMOs are of Cr-d + O-p character, except for Cr_7Cu, where LUMO stems from the Cu d orbitals. This is particularly evident in Figure 5, where the spatial distribution of the orbitals with energy around the HOMO−LUMO gap is presented as three-dimensional contour plots of isosurfaces of value ±0.05; we have here plotted all the levels which are within 0.1 eV from the HOMO and LUMO levels. If HOMO states are attained at well-isolated energy levels, with well-defined spin character (reported in Figure 5), several spin unpolarized unoccupied orbital states, i.e., LUMO+1, LUMO+2, and so forth, can be found very close in energy to the LUMO state, except for Cr_7Cu. The HOMO states are well localized at the divalent substituting atom M and have a predominantly d character, and this holds for all the molecules studied here. Nominal electronic configuration of Ni^{2+}, Mn^{2+}, Fe^{2+}, and Cu^{2+} are respectively d^8, d^5, d^6, and d^9. In the case of Ni and Cu, the 3d shell is nearly filled, and the energy splitting between the occupied majority and minority spins is reduced; this leads to orbitals of both spins close to the highest occupied one, which has d_{z^2} e_g-like spin ↓ and $d_{x^2-y^2}$ e_g-like spin ↑ character for Cr_7Ni and Cr_7Cu, respectively. Mn^{2+} has one spin channel fully occupied, and its highest occupied orbital has d_{z^2} e_g-like character, and spin ↑ character. Fe has only one occupied minority spin orbital: the HOMO turns out to have a d_{xy} t_{2g}-like spin ↓ character. The bunch of (almost non spin-polarized) LUMO states in the low-energy region near the conduction minimum have Cr-d and O-p character, except for Cr_7Cu, and are spatially pinpointed to the ring region opposite to the divalent substituting atom.

Before proceeding further with the discussion, we comment on the approximations involved in our calculations. The prediction of electronic gaps in correlated solid state and molecular materials is known to be a difficult task. Standard local functionals systematically underestimate the gaps. LDA+U calculations, which takes into account with an adjustable parameter *U* static correlation effects beyond LDA, is known to sensibly improve the comparison with experiments. The choice of the *U* parameter is not trivial, although in the case of oxygen-coordinated transition metal ions, the behavior can be matched to the one of the parent oxide bulk compounds; for example, for Cr_7Ni, with Cr^{3+} and Ni^{2+} valencies, a logical choice for U_{Cr} and U_{Ni} would be to use the values assumed in oxide compounds with equal valencies, such as Cr_2O_3 and NiO. Hybrid functionals, as the one used in this paper, avoid the uncertainty of having element-dependent *U* parameters, and supply an unique parametrization that is universally applicable. The B3LYP functional used throughout this paper "contains" more correlation than LDA or GGA, and while it is generally accepted as the most trustful choice for the studies of coordination clusters, it has been shown in strong correlated bulk compounds to behave similarly to the LDA+U method concerning electronic gaps and the electronic properties in general.[32−34] The reduced gap for Cr_7Mn and Cr_7Fe is therefore likely to be of real physical origin.

Spin States of the Charged Molecules. Let us focus, for the time being, on Cr_7Ni, which is the molecule, among the Cr_7M rings, most studied in the literature. In order to read, or modify, the spin state of a single molecule magnet, a viable approach is to exert a local electric field, for instance with a scanning tunneling microscope (STM) tip. Recently Misiorny et al.[43] have suggested that a spin-polarized current could be employed in order to switch the spin of the molecule, by supposing that the current flows via the LUMO and is exchange-coupled to the total spin of the molecule. The influence of an additional electron (or hole, in the case of hole-transport) on the magnetic properties of a single-molecule magnet (SMM) is therefore of critical importance. We have performed total energy calculation in the presence of an additional charge, and considered both the case where the additional electron has spin up or spin down with respect to the total spin of the ring. In agreement with the observation of Barraza-Lopez et al.,[23] the ground state of $(Cr_7Ni)^-$ is characterized by the a total spin $S = S^0 + 1/2$, where S^0 is the spin of the uncharged Cr_7Ni ($S^0 = 1/2$); total energy calculations predict that the $S = 1$ spin state is 16.7 meV lower in energy than the $S = 0$ spin state, i.e., the spin of the additional e^- is preferentially aligned to the total spin of the molecule. An analysis of the HOMO orbital in the charged state, shows that the additional electron is delocalized over several Cr atoms (and on their coordination F and O atoms), which is, by the

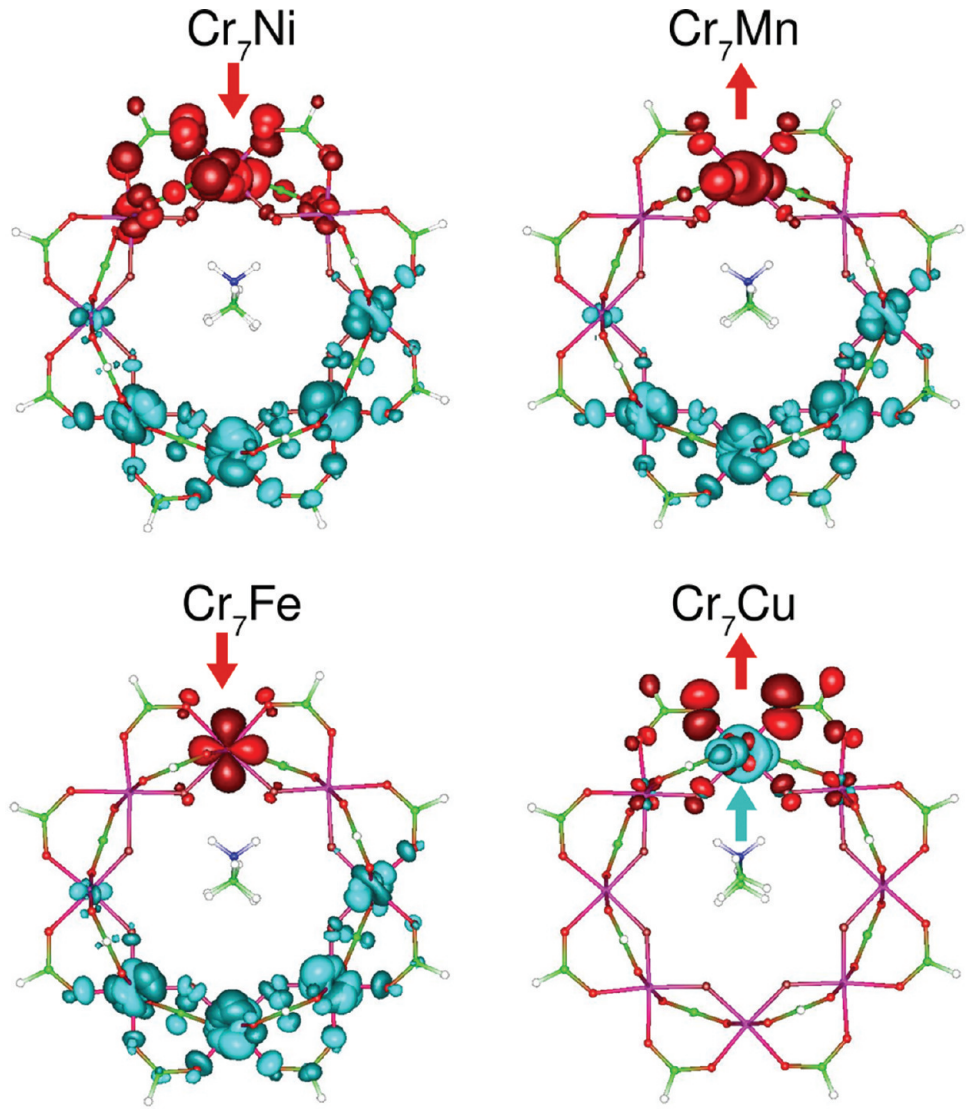

Figure 5. Isosurface plots of the HOMO (red) and LUMO (cyan) levels in Cr_7M, M = Ni, Mn, Fe, and Cu rings of derivative **2** in the AFM state, for isovalues of ±0.05/a.u. The colored arrows (when present) indicate the predominant spin channel of the HOMO/LUMO levels as compared to the total spin of the molecule; orbitals with energy that fall in the [HOMO-0.1 eV: HOMO] and [LUMO: LUMO+0.1 eV] energy windows are plotted.

way, already evident by looking at the spatial distribution of the LUMO state in the neutral molecule (see Figure 5). Such delocalization favors in general an increase in the total magnetic moment of the molecule, in the case of homometallic clusters, while electron doping coming from inner atomic substitution, as discussed in ref 23 would modify the spin of the molecule differently depending on the magnetic moment of the atoms that accommodate the additional electron by the reduction mechanism. This mechanism in the case of heterometallic species is not straightforward. In fact, as anticipated in the paragraph where we discussed the orbital and spin character of the HOMO and LUMO levels, in all cases, except Cr_7Cu, we are in the presence of LUMO levels which are delocalized over a large portion of the ring, and with an almost spin-unpolarized character; yet a small polarization is found, and its sign is mainly determined by the Cr magnetic moment opposite to the M atom, with respect to the octagon. In the case of Cr_7Ni, the lowest LUMO levels belong to the (↑) channel, and the additional electron increases the total spin moment of the molecule, as observed in the calculation; for Cr_7Mn and Cr_7Fe, instead, an additional electron will decrease the total spin of the molecule. Cr_7Cu is a case on its own, and the additional electron is predicted to localize on the Cu atom, switching off its spin.

On the Charge Transport in the Resonant-Tunneling Regime. The different aspects of the electronic properties of the Cr_7M rings presented in the previous sections, as a function of the substituting dication, offer interesting cues from which conjectures on their transport behavior and on how one can exploit them in order to image them or knowing how they orient in a junction, can be set. Considering the size of the ligands, such as thiophene or phenoxybenzoate, used in ref 12 when grafting Cr_7Ni molecules on gold surfaces, we can assume that tunneling experiments through such functionalized derivatives take place in the resonant tunneling (low-coupling) regime, where electrons can tunnel on and off the molecule, and where the conductance can be directly related to the energy level spectrum of the molecule and to the knowledge of the spatial delocalization of the various energy channels. Recent scanning tunneling spectroscopy experiments on Mn_{12} SMM have estimated, from the asymmetric behavior of the current versus applied voltage, as a function of the set voltage, that tunneling involves mainly HOMO states,[44] although the existence of

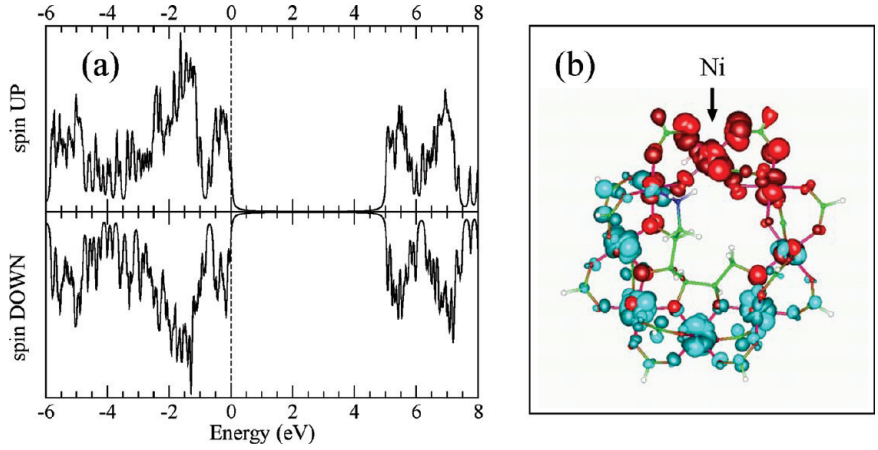

Figure 6. (a) Spin-polarized total DOS and (b) isosurface plots of the HOMO (red) and LUMO (cyan) levels in the Cr_7Ni ring of derivative **3** in the AFM state, for isovalues of ±0.05/a.u. Orbitals with energy that fall in the [HOMO-0.1 eV: HOMO] and [LUMO: LUMO+0.1 eV] energy windows are plotted; the position of the Ni atom is indicated with a black arrow.

unaltered Mn_{12} molecules when grafted on a surface has been seriously questioned.[45] The firm character of the HOMO states, localized on the substituted divalent M^{2+} atom, would in principle lead to a dependence of the tunneling current on the relative orientation of the ring cycle with respect to the leads in a molecular junction geometry. This localization can in fact result in a suppressed current, while more delocalized LUMO might transmit large currents, leading to a strong asymmetry with respect to the sign of the applied voltage.

How will the underlying AFM structure show up in transport experiments? To tackle this question, we also comment on the possibility that sequential tunneling, as proposed by Lehmann and Loss in ref 22 may depend on the geometry of the contacts with respect to the AFM structure of a spin ring. They propose that the current for low bias can be completely suppressed upon contacting magnetic ions that are antiferromagnetically coupled in the ground state, while this might not be the case when contacting atoms that are ferromagnetically coupled. Although their calculations hold for a ring of four ions with more than half-filled magnetic orbitals (e.g., a ring of four Fe^{3+} ions), the idea seems to be generally applicable. In fact it has been shown that a similar breakdown of the current (coulomb-blockade) is predicted for a benzene ring, where the transport channels are supplied by π electrons.[46] In the case of the spin ring, the spatial localization of the orbital that allows transport is connected to the spin alternation on the ions, while in the case of the benzene ring it comes from the symmetry of the orbitals involved and from the positive−negative interference mechanism associated with the delocalization of the π electron system.[47,48] In the case of a heterometallic ring, such as Cr_7M, the asymmetry induced by the substituting atom superimposes its form to such alternation, and LUMO states that might host the electron hopping from the leads are localized mainly on one side of the ring. A different behavior of the transport upon contacting the molecule on different sides of the ring would thus be more difficult to trace back to the underlying spin distribution only. In the case of the parent Cr_8 molecule, instead this would still be possible, although in reality direct access to a magnetic ion is difficult to achieve, because of the bulky organic ligands that chelate the inner magnetic core.

The main metallic character of the HOMO and LUMO, which seems to be a general finding in molecular magnets, and their energy separation from the ligand levels can also be exploited in STM experiments to study the orientation of a molecule on a surface.[49] By tuning the gate voltage, the metallic d orbital levels can be pinpointed to the drain-source energy window and lead to resonant tunneling; in this way, the two-dimensional arrangement of the metallic ions show up as bright spots in the STM image (for a recent review, see ref 50). We suggest that the planar octagonal arrangement of the Cr and M atoms in the cyclic rings of interest can similarly be visualized, allowing one in principle to discern between planar and perpendicular arrangement of the cycles with respect to the surface plane. In the case of planar arrangement, the same property can be exploited to discern the position of the M site in the ring, which in Cr_7M crystals is undetermined since the M site is disordered over all possible metal sites (this degeneracy is lifted in the "purple" rings by the presence of the glucamine bridging ligands, see Figure 1b). The separation in energy between the HOMO states of the M and Cr atoms, which, e.g., in Cr_7Ni is on the order of 1 eV, can be used as follows: Setting the bias voltage so that only levels close to the HOMO are probed will allow one to spot the position of the Ni atom within the cycle.

Cr_7Ni Molecular Ring of Derivative 3. We now report on the calculations of the electronic and magnetic properties of the Cr_7Ni ring of derivative **3**, in order to illustrate how structural differences between the two derivatives influence their properties. As anticipated before, only Ni substitution has been achieved by synthesis so far, and we restrict our analysis for the time being on this specific ring only. In Figure 6 we show the total DOS (panel a) and isosurface plot of HOMOs and LUMOs (panel b) of the "purple" Cr_7Ni ring; similarly to Figure 5, because of the energetic proximity of several states, we include in the plot all the orbitals whose energies belong to the [HOMO-0.1 eV: HOMO] and [LUMO: LUMO+0.1 eV] energy windows, as done in the case of derivative **2**. The analysis of the DOS reveal that, as opposed to the Cr_7Ni of derivative **2**, Ni- and Cr-occupied d orbitals (hybridized with p states of the neighboring atoms) are not separated in energy (compare Figure 6a and Figure 4 top-left panel); as a consequence, the HOMO is not localized on the Ni atoms but spreads over a larger portion of the molecule (red isosurface in Figure 6b). On the other hand LUMOs have mainly Cr character, as in derivative **2**, and orbitals are delocalized over half of the ring, the one individuated by the glucamine bridge. The discussion of the previous section, applies only in part for the derivative **3**, since both HOMO and LUMO are more delocalized, and d orbitals of Cr and Ni overlap in energy, so that the energy filtering mechanism described in the previous section, used to discern the position of Ni ions, might not be feasible. On the other hand, metallic sites might

still be located, and the distortion of the octagon can help in recognizing the position of the glucamine ligands, and, consequently, of the Ni ions. Moreover, since both HOMOs and LUMOs have no clear spin character, electrons flowing through this molecule might "experience" only the electronic degrees of freedom. Notwithstanding the large modifications in the molecule, with special regard on the glucamine bridge, which replaces five F bridges, i.e., replacing one out of three bridges that mediate the interaction between two Cr ions, the magnetic interactions between the paramagnetic ions has been found to be similar to the ones observed in the derivative **2**. More precisely, Heisenberg exchange parameters $J_{Cr-Cr} = J_{Cr-Ni} =$ 2.0 meV have been obtained by fitting temperature-dependent susceptibility,[9] which thus implies only a slightly larger AFM coupling between magnetic ions as compared to derivative **2**, where $J_{Cr-Cr} = J_{Cr-Ni} = 1.5$ meV. By applying the total energy difference procedure described earlier, we find values of 3.9 and 2.0 meV, respectively, for J_{Cr-Cr} and J_{Cr-Ni}, on the line of the experimental findings. The HOMO−LUMO gap is calculated to be 5.0 meV, which is slightly larger than the one of the "green" Cr_7Ni ring (4.2 meV).

Conclusions

We have presented an extensive analysis of the electronic and magnetic properties of two different derivatives of substituted Cr_7M rings, with M = divalent magnetic ion, such as Ni^{2+}, Fe^{2+}, Mn^{2+}, or Cu^{2+}. Exchange interaction parameters extracted for rings of both derivatives are overestimated by a factor of 2 with respect to the experimental values, as expected from the adoption of the projected BS method and B3LYP functionals; some variation is also observed in the exchange parameters relative to the Cr−M interactions, as a function of M, a fact that is not observed in experiments. On the other hand, magnetic properties of Cr_7Ni rings belonging to the two derivatives are rather similar, despite the difference in the bridging ligands that mediate the magnetic interactions, in agreement with the experiments. The analysis of the electronic properties, suggest that, in the case of transport events, in the resonant tunneling regime, the localization of the HOMO orbital on the substituting atom would suppress the tunneling current, while LUMO-mediated electron transport would be more likely to occur due to larger orbital delocalization. On the basis of these results, we predict a large asymmetry in the current depending on the sign of the applied voltage. Moreover, the firm metallic character of the states composing the HOMOs and the LUMOs can be exploited to discern how the molecules are arranged on a surface, and pinpoint the position of the substituting M ions, by selecting the resonant channels by bias voltage tuning in STM experiments.

Acknowledgment. We acknowledge fruitful discussion with G. Timco, R. E. P. Winpenny, F. Troiani, A. Ghirri, V. Corradini, and D. Vanossi. The calculations were performed on computer facilities granted by the CNR-INFM *Iniziativa Trasversale Calcolo Parallelo* at the CINECA supercomputing center. We aknowledge the support from the EU NoE-MAGMANET Contract No. NMP3-CT-2005-515767 and the European Project FP7-ICT FET Open "MolSpinQIP" project, Contract No. 211284.

References and Notes

(1) Sessoli, R.; Gatteschi, D.; Caneschi, A.; Novak, M. A. *Nature* **1993**, *365*, 141.
(2) Ardavan, A.; Rival, O.; Morton, J. J.; Blundell, S. J.; Tyryshkin, A. M.; Timco, G. A.; Winpenny, R. E. P. *Phys. Rev. Lett.* **2007**, *98*, 057201.
(3) Leuenberger, M. L.; Loss, D. *Nature* **2001**, *410*, 789.
(4) Meier, F.; Levy, J.; Loss, D. *Phys. Rev. Lett.* **2003**, *90*, 047901.
(5) Troiani, F.; Affronte, M.; Carretta, S.; Santini, P.; Amoretti, G. *Phys. Rev. Lett.* **2005**, *94*, 190501.
(6) Troiani, F.; Ghirri, A.; Affronte, M.; Carretta, S.; Santini, P.; Amoretti, G.; Piligkos, S.; Timco, G.; Winpenny, R. E. P. *Phys. Rev. Lett.* **2005**, *94*, 207208.
(7) Affronte, M.; Carretta, S.; Timco, G. A.; Winpenny, R. E. P. *Chem. Commun.* **2007**, *18*, 1789.
(8) Timco, G. A.; Carretta, S.; Troiani, F.; Tuna, F.; Pritchard, R. J.; Muryn, C. A.; McInnes, E. J. L.; Ghirri, A.; Candini, A.; Santini, P.; Amoretti, G.; Affronte, M.; Winpenny, R. E. P. *Nature Nanotechnol.* **2009**, *4*, 173.
(9) Candini, A.; Lorusso, G.; Troiani, F.; Ghirri, A.; Carretta, S.; Santini, P.; Amoretti, G.; Muryn, M. C.; Tuna, F.; Timco, G.; McInnes, E. J. L.; Winpenny, R. E. P.; Wernsdorfer, W.; Affronte, M. *Phys. Ref. Lett.* **2010**, *104*, 037203.
(10) McInnes, E. J. L.; Piligkos, S.; Timco, G. A.; Winpenny, R. E. P. *Coord. Chem. Rev.* **2005**, *249*, 2577.
(11) van Slageren, J.; Sessoli, R.; Gatteschi, D.; Smith, A. A.; Helliwell, M.; Winpenny, R. E. P.; Cornia, A.; Barra, A. L.; Jansen, A. G. M.; Rentschler, E.; Timco, G. A. *Chem.—Eur. J.* **2002**, *8*, 277.
(12) Corradini, V.; Moro, F.; Biagi, R.; del Pennino, U.; Renzi, V. D.; Carretta, S.; Santini, P.; Affronte, M.; Cezar, J. C.; Timco, G. A.; Winpenny, R. E. P. *Phys. Rev. B* **2008**, *77*, 014402.
(13) Corradini, V.; Moro, F.; Biagi, R.; De Renzi, V.; del Pennino, U.; Bellini, V.; Carretta, S.; Santini, P.; Milway, V.; Timco, G.; Winpenny, R.; Affronte, M. *Phys. Rev. B* **2009**, *79*, 144419.
(14) Carretta, S.; van Slageren, J.; Guidi, T.; Liviotti, E.; Mondelli, C.; Rovai, D.; Cornia, A.; Dearden, A. L.; Carsughi, F.; Frost, M. A. C. D.; Winpenny, R. E. P.; Gatteschi, D.; Amoretti, G.; Caciuffo, R. *Phys. Rev. B* **2003**, *67*, 94405.
(15) Caciuffo, R.; Guidi, T.; Amoretti, G.; Carretta, S.; Liviotti, E.; Santini, P.; Mondelli, C.; Timco, G.; Muryn, C. A.; Winpenny, R. E. P. *Phys. Rev. B* **2005**, *71*, 174407.
(16) Engelhardt, L. P.; Muryn, C. A.; Pritchard, R. G.; Timco, G. A.; Tuna, F.; Winpenny, R. E. P. *Angew. Chem., Int. Ed.* **2008**, *47*, 924.
(17) Amiri, H.; Mariani, M.; Lascialfari, A.; Borsa, F.; Timco, G. A.; Tuna, F.; Winpenny, R. E. P. *Phys. Rev. B* **2010**, *81*, 104408.
(18) Bellini, V.; Olivieri, A.; Manghi, F. *Phys. Rev. B* **2006**, *73*, 184431.
(19) Troiani, F.; Bellini, V.; Affronte, M. *Phys. Rev. B* **2008**, *77*, 054428.
(20) Blaha, P.; Schwarz, K.; Madsen, G.; Kvasnicka, D.; Luitz, J. *WIEN2k, An Augmented Plane Wave + Local Orbitals Program for Calculating Crystal Properties*; Karlheinz Schwarz, Techn. Universität Wien: Austria, 2001; ISBN 3-9501031-1-2.
(21) Tomecka, D.; Bellini, V.; Troiani, F.; Manghi, F.; Affronte, M.; Kamieniarz, G. *Phys. Rev. B* **2008**, *77*, 224401.
(22) Lehmann, J.; Loss, D. *Phys. Rev. Lett.* **2007**, *98*, 117203.
(23) Barraza-Lopez, S.; Park, K.; García-Suárez, V.; Ferrer, J. *Phys. Rev. Lett.* **2009**, *102*, 246801.
(24) Valiev, M.; Bylaska, E. J.; Govind, N.; Kowalski, K.; Straatsma, T. P.; van Dam, H. J. J.; Wang, D.; Nieplocha, J.; Apra, E.; Windus, T. L.; de Jong, W. A. NWChem: a comprehensive and scalable open-source solution for large scale molecular simulations; *Comput. Phys. Commun.* **2010**, *181*, 1477.
(25) Timco, G. A.; McInnes, E. J. L.; Pritchard, R. J.; Tuna, F.; Winpenny, R. E. P. *Angew. Chem., Int. Ed.* **2008**, *47*, 9681.
(26) Larsen, F. K.; McInnes, E. J. L.; Mkami, H. E.; Overgaard, J.; Piligkos, S.; Rajaraman, G.; Rentschler, E.; Smith, A. A.; Smith, G. M.; Boote, V.; Jennings, M.; Timco, G. A.; Winpenny, R. E. P. *Angew. Chem., Int. Ed.* **2003**, *42*, 101.
(27) Anisimov, V. I.; Solovyev, I. V.; Korotin, M. A.; Czyzyk, M. T.; Sawatzky, G. A. *Phys. Rev. B* **1993**, *48*, 16929.
(28) Liechtenstein, A. I.; Anisimov, V. I.; Zaanen, J. *Phys. Rev. B* **1995**, *52*, R5467.
(29) Boukhvalov, D. W.; Lichtenstein, A. I.; Dobrovitski, V. V.; Katsnelson, M. I.; Harmon, B. N.; Mazurenko, V. V.; Anisimov, V. I. *Phys. Rev. B* **2002**, *65*, 184435.
(30) Postnikov, A. V.; Bihlmayer, G.; Blügel, S. *Inorg. Chem.* **2004**, *43*, 5053.
(31) Schafer, A.; Horn, H.; Ahlrichs, R. *J. Chem. Phys.* **1992**, *97*, 2571.
(32) Franchini, C.; Bayer, V.; Poudloucky, R. *Phys. Rev. B* **2005**, *72*, 045132.
(33) Grau-Crespo, R.; Corá, F.; Sokol, A. A.; de Leeuw, N. H.; Catlow, C. R. A. *Phys. Rev. B* **2006**, *73*, 035116.
(34) Tran, F.; Blaha, P.; Schwarz, K.; Novák, P. *Phys. Rev. B* **2006**, *74*, 155108.
(35) Wu, Q.; van Voorhis, T. *Phys. Rev. A* **2005**, *72*, 024502.
(36) Rudra, I.; van Voorhis, T. *J. Chem. Phys.* **2006**, *124*, 024103.
(37) Ruiz, E. *Struct. Bonding* **2004**, *113*, 71.
(38) Neese, F. *J. Chem. Phys.* **2001**, *115*, 11080.
(39) Rivero, P.; Loschen, C.; Moreira, I.; Illas, F. *J. Comput. Chem.* **2009**, *30*, 2316.

(40) We considered only the Fermi contact term by means of the relativistic Breit formula.[52]

(41) Bellini, V.; Tomecka, D.; Manghi, F.; Affronte, M.; Kamieniarz, G. To be published (2010).

(42) Rudra, I.; Wu, Q.; van Voorhis, T. *Inorg. Chem.* **2007**, *46*, 10539.

(43) Misiorny, M.; Barnaś, J. *Phys. Rev. B* **2007**, *76*, 054448.

(44) Voss, S.; Zander, O.; Fonin, M.; Rüdiger, U.; Burgert, M.; Groth, U. *Phys. Rev. B* **2008**, *78*, 155403.

(45) Mannini, M.; Sainctavit, P.; Sessoli, R.; CartierditMoulin, C.; Pineider, F.; Arrio, M.; Cornia, A.; Gatteschi, D. *Chem.—Eur. J.* **2008**, *14*, 7530.

(46) Hettler, M. H.; Wenzel, W.; Wegewijs, M. R.; Schoeller, H. *Phys. Rev. Lett.* **2003**, *90*, 076805.

(47) Richardson, D. E.; Taube, H. *J. Am. Chem. Soc*. **1983**, *105*, 40.

(48) Marvaud, V.; Launay, J.-P.; Joachim, C. *Chem. Phys.* **1993**, *177*, 23.

(49) Vitali, L.; Fabris, S.; Mosca conte, A.; Brink, S.; Ruben, M.; Baroni, S.; Kern, K. *Nano Lett.* **2008**, *8*, 3364.

(50) Petukhov, K.; Alam, M. S.; Rupp, H.; Strömsdörfer, S.; Müller, P.; Scheurer, A.; Saalfrank, R. W.; Kortus, J.; Postnikov, A.; Ruben, M.; Thompson, L. K.; Lehn, J.-M. *Coord. Chem. Rev.* **2009**, *253*, 2387.

(51) Allalen, M.; Schnack, J. *J. Magn. Magn. Mater.* **2006**, *302*, 206.

(52) Breit, G. *Phys. Rev.* **1930**, *35*, 1447.

JP107544Z